

Focusing of medium-energy electrons upon quasielastic reflection from a crystal

M. V. Gomoyunova, I. I. Pronin, and N. S. Faradzhev

A. F. Ioffe Physicotechnical Institute, Russian Academy of Sciences, 194021 St. Petersburg, Russia

(Submitted 8 December 1995)

Zh. Éksp. Teor. Fiz. **110**, 311–321 (July 1996)

We study the mechanism underlying the formation of the Kikuchi patterns observed when the complete spatial distributions of medium-energy electrons quasielastically reflected from a thin near-surface layer of a crystal are recorded. Measurements are made for Mo(110) in the energy range 0.8–2 keV. Model calculations performed on the basis of the focusing of electrons in a crystal faithfully describe the experiment. It is shown that higher-order diffraction maxima scarcely play a role at an energy of 2 keV; therefore, the corresponding Kikuchi patterns, reflecting interatomic directions, make it possible to visualize the relative positions of the atoms in several monatomic layers of the solid. © 1996 American Institute of Physics. [S1063-7761(96)02307-4]

1. INTRODUCTION

In recent years there has been a notable revival of research on the Kikuchi patterns^{1–7} observed when the complete spatial distributions of electrons reflected inelastically by the near-surface layers of a crystal are recorded. The heightened interest in this problem is due, on the one hand, to the appearance of a new theory of these patterns and, on the other hand, to the bright prospects for their utilization in the structural analysis of the surfaces of solids.

One characteristic feature of the diffraction patterns under consideration is the enhancement of the reflection of electrons along densely packed crystal planes (Kikuchi bands).^{8–14} The traditional explanation of these bands treats the formation of the patterns as a two-stage process. In the first, diffuse inelastic scattering of the primary electrons takes place (“internal” sources of reflected electrons appear), and in the second, they undergo diffraction on the planes of the semi-infinite crystal. A detailed investigation of the spatial distributions¹² of quasielastically scattered electrons appearing only as a result of interactions with phonons demonstrated the key role of densely packed rows of atoms in the crystal in the formation of the patterns.

A new mechanism,^{1,15} which relates the predominant reflection of electrons along rows of atoms to forward focusing of the electrons as they move in the crystal, was proposed to describe the second stage of the process under consideration. This effect also has a diffraction mechanism. It is attributable to interference between the primary wave propagating from a point source in the crystal and the waves that emerge when it is scattered by the atoms surrounding that source. Focusing is observed at electron energies exceeding several hundred electron-volts, at which there is already strong forward peaking of the electron–atom scattering diagram. The effect is especially pronounced in the spatial distributions of fast photoelectrons and Auger electrons, which are now widely used to investigate the local atomic structure of the surfaces of solids.^{15–17} The extent to which the theories on the focusing of electrons in a crystal are sufficient for faithfully describing Kikuchi patterns and using them in structural analysis has

not yet been determined. The present work was undertaken to clarify this question.

For this purpose Kikuchi patterns created only by quasielastically scattered electrons were thoroughly investigated. This enables us to study the phenomenon in its simplest form without including the reflected continuum electrons, with energy losses up to tens of electron-volts, which are usually recorded together with the quasielastically scattered electrons. The investigation is carried out on a Mo(110) single crystal whose surface was not reconstructed and whose atomic structure was reliably established. The experimental results are compared with calculations performed in the plane-wave approximation of the single-scattering cluster model. It is shown that despite the roughness of the approximation used, the calculations performed without fitting parameters faithfully describe the Kikuchi pattern. Moreover, it is demonstrated that a highly simplified model that phenomenologically takes into account the focusing of electrons only on isolated scattering atoms is also consistent with experiment, and can be used in practical applications of Kikuchi patterns for the structural analysis of surfaces. The main result of this work is confirmation that all of the basic features are determined by the focusing of quasielastically scattered electrons along interatomic directions of the crystal, which enables us to use Kikuchi patterns to visualize the relative positions of atoms in the near-surface layers of a solid.

2. EXPERIMENTAL METHOD

To investigate the Kikuchi patterns, the intensity I of the elastic reflection peak of the electrons was measured in this work as a function of the polar (θ) and azimuthal (φ) emission angles of the electrons. Due to the inadequate energy resolution of existing spectrometers at energies exceeding hundreds of electron-volts, this procedure leads to the combined detection of electrons that have undergone both elastic scattering from the periodic potential of the lattice of the solid and quasielastic scattering. The relative contributions of these groups to the measured signal depend on the energy. The fraction of purely elastic scattering decreases with increasing energy and becomes small when $E > 1$ eV, making

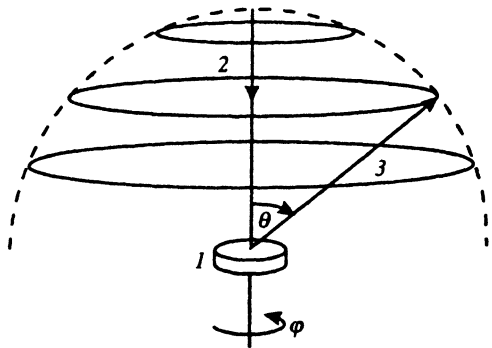


FIG. 1. Experimental setup: 1 — sample, 2 — beam of primary electrons, 3 — beam of electrons being detected.

it possible to obtain the desired diffraction patterns. One advantage of recording the elastic reflection peak instead of other portions of the spectrum of reflected electrons (for example, electrons that have lost energy to excite plasmons) is the higher sensitivity of the pattern to the state of the surface of the sample, due to the shorter escape length of the electrons under consideration. We also note that the high intensity of the signal of the quasielastically scattered electrons is sufficient for recording Kikuchi patterns under real-time conditions, making it possible to investigate various atomic processes occurring on the surface.

Measurements in the energy range $E=0.8-2$ keV were performed on an original ultrahigh-vacuum secondary-ion spectrometer, which was described in detail in Ref. 18. The quasielastically scattered electrons were detected by a channel electron multiplier, which was positioned at the output of an electrostatic energy analyzer of the modified flat mirror type. The energy resolution of the analyzer was 0.4%, and its angular resolution was 1° . The amplitude of the peak in the spectrum was measured by modulating the current of primary electrons, which was usually 20 nA. The polar emission angle of the detected electrons was varied by rotating the energy analyzer about the sample, and the azimuthal angle was varied by rotating the crystal about an axis perpendicular to its surface (Fig. 1). Thus, under normal incidence of the primary beam, the spectrometer permitted automatic recording of the spatial distributions of the electrons over a broad range of emission angles: $\theta=18^\circ-85^\circ$, $\varphi=0^\circ-360^\circ$. The most detailed data of this kind (with spacing of 1° in both angles) were obtained in the present work for the highest energy allowed for the instrument, which is 2 keV, and at which the Kikuchi pattern of the Mo(110) surface shows up most strongly.

The Mo(110) sample had a diameter of 12 mm. It was cut from a single crystal obtained by zone melting, burnished, and electrolytically polished to mirror brightness. The accuracy of exposing the face on the surface was better than 1° . The sample surface was cleaned to remove any carbonaceous contaminants, sulfur, and oxygen using a standard method by alternately heating the crystal in an oxygen atmosphere at a pressure $p=10^{-6}$ Torr and in a vacuum with a residual pressure $p<10^{-9}$ Torr at 2300 K. The elemental composition of the surface was monitored by Auger electron

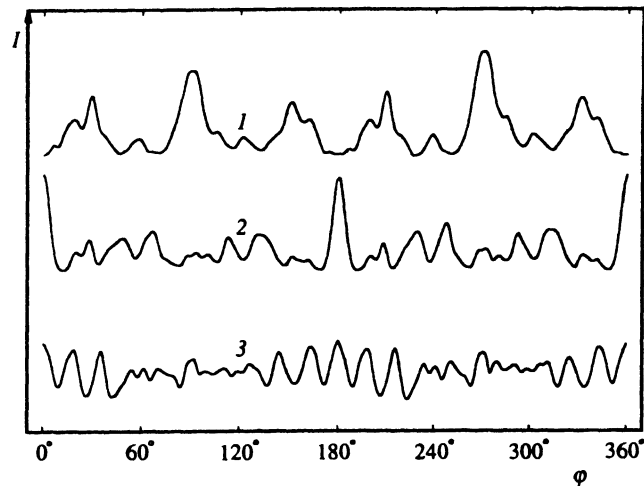


FIG. 2. Azimuthal angular distributions of electrons with an energy of 2 keV quasielastically reflected from Mo(110) for polar emission angles of the electrons equal to 35° (1), 45° (2), and 65° (3).

spectroscopy, and after cleaning, the content of the impurities (carbon) did not exceed 10% of a monolayer. The atomic structure of the sample surface was monitored by low-energy electron diffraction (LEED). A clear $p(1\times 1)$ pattern was observed, attesting to the structural ordering of the upper layers of the crystal and the correspondence of their structure to the bulk. The measurements were performed at room temperature in a 5×10^{-10} Torr vacuum.

3. KIKUCHI PATTERN OF Mo(110)

The diffraction of reflected electrons is manifested most vividly by the anisotropy of their distributions $I(\varphi)$ in azimuthal emission angle. The nonmonotonic character of these dependences also unequivocally attests to the structural ordering of the near-surface layers of the sample. Typical plots of $I(\varphi)$ for Mo(110), which illustrate the primary experimental data for an energy of 2 keV, are shown in Fig. 2. Their maximum anisotropy reaches 57% at a polar angle of 35° . The anisotropy was evaluated using the parameter $\chi=[(I_{\max}-I_{\min})/I_{\max}]\cdot 100\%$, where I_{\max} and I_{\min} are the maximum and minimum values of the intensity $I(\varphi)$. Due to the symmetry of the Mo(110) face, the distributions have a period of 180° and exhibit mirror symmetry relative to the $\varphi=90^\circ$ (270°) plane. The deviations from symmetry are negligible.

A complete Kikuchi pattern of Mo(110), which sums all the data obtained at $E=2$ keV, is shown in Fig. 3a. It is represented in the form of a two-dimensional map of the distribution of the intensity $I(\theta, \varphi)$ of the quasielastic scattering with respect to the polar and azimuthal emission angles and is presented in a stereographic projection. The center of the circle corresponds to a normal to the surface, and the outer circle corresponds to the emission of electrons along the surface. The pattern is depicted in a linear scale of gray tones, in which white corresponds to maximum reflection and black corresponds to minimum reflection. In constructing the Kikuchi pattern each azimuthal scan of $I(\varphi)$ was normalized to the mean value of its intensity, making it

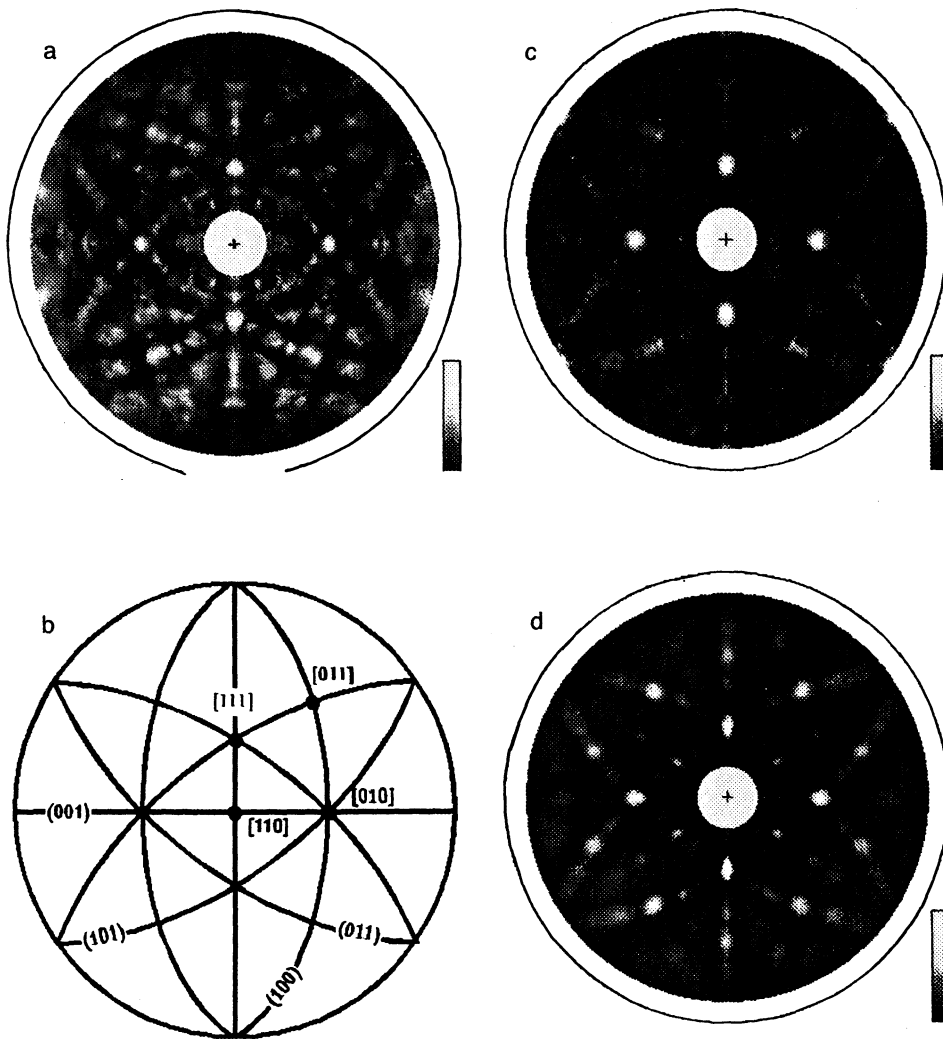


FIG. 3. a — Kikuchi pattern of Mo(110) created by quasielastically scattered electrons with an energy of 2 keV represented in a stereographic projection. b — Principal planes and densely packed directions in the crystal. c — Calculated Mo(110) Kikuchi pattern obtained in the plane-wave approximation of the single-scattering cluster model. d — Calculated Kikuchi pattern obtained in a cluster model that phenomenologically takes into account the focusing of electrons.

possible to eliminate the distorting influence of the instrumental function of the spectrometer, which underestimates the intensity of the electrons detected at large θ .

The pattern clearly displays regions of enhanced emission intensity, which form Kikuchi bands oriented obliquely and perpendicularly to the surface of the sample. The strongest reflection maxima are observed where these bands intersect. The identification of these features of the diffraction pattern with specific crystallographic directions and planes is given in Fig. 3b, which also depicts the most densely packed directions and planes for a bcc (110) face in the same stereographic projection. A comparison of Figs. 3a and 3b reveals agreement between the principal maxima of $I(\theta, \varphi)$ and the lowest-index directions of the crystal. In particular, strong maxima are clearly seen in the $\langle 111 \rangle$, $\langle 100 \rangle$, and $\langle 110 \rangle$ directions. Similarly, the bands of enhanced reflection intensity are oriented in the projections of the $\{110\}$, $\{100\}$, and $\{111\}$ planes.

4. SIMULATION OF A KIKUCHI PATTERN IN THE SINGLE-SCATTERING CLUSTER APPROXIMATION

Relying on the well-known commonality of Kikuchi patterns and the diffraction patterns of fast Auger and

photoelectrons,¹¹ which are described well in many cases by the single-scattering cluster approximation, we used this approach to numerically simulate the complete Kikuchi pattern of Mo(110). The model was modified with consideration of the details of quasielastic scattering of electrons by a crystal.

The starting point was the assumption that isotropic sources of scattered electronic waves localized on crystal-lattice sites appear in the near-surface layer of the crystal in the first stage of the process. The probability of the excitation of these sources was assumed to decay z_i with depth as $\exp(-z_i/\lambda)$, where λ is the mean free path of the primary electrons before inelastic scattering. The value of λ was calculated using the generally accepted Seah equation¹⁹ and was equal to 23 Å.

The second stage of the process, i.e., the focusing of the electrons emitted by these sources and their interaction with the atoms surrounding the emitter as they leave the crystal, was treated in the plane-wave approximation. The required data on the scattering amplitudes $f_j(\theta_j)$ and the phase shifts $\gamma_j(\theta_j)$ were taken from Fink's tables.²⁰ Since the latter were restricted to an energy of 1.5 keV, they were extrapolated to 2 keV. The contributions $I_i(\theta, \varphi)$ from the individual sources to the total intensity of the Kikuchi pattern in the recording

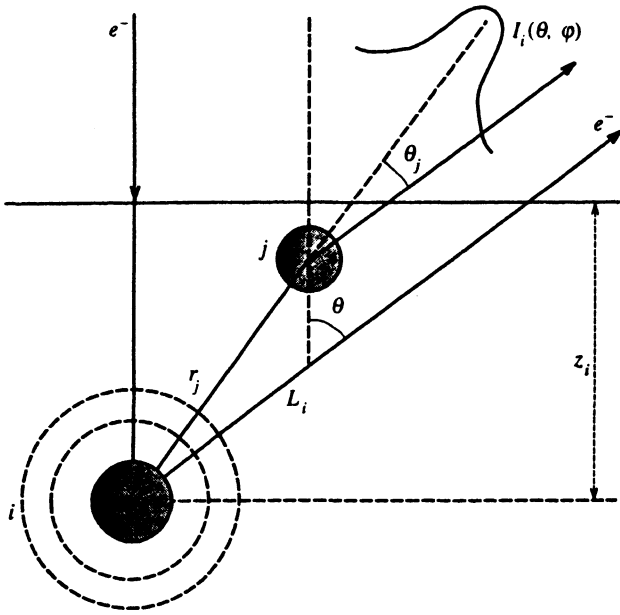


FIG. 4. Diagram explaining the single-scattering cluster model.

direction were calculated in the standard manner:¹⁷

$$I_i(\theta, \varphi) \propto \left| \exp\left(-\frac{L_i}{2\lambda}\right) + \sum_j \frac{|f_j(\theta_j)|}{r_j} W_j \exp\left(-\frac{L_j}{2\lambda}\right) \times \exp\{i[kr_j(1 - \cos \theta_j) + \gamma_j(\theta_j)]\} \right|^2 + \sum_j \frac{|f_j(\theta_j)|^2}{r_j^2} (1 - W_j^2) \exp\left(-\frac{L_j}{\lambda}\right). \quad (1)$$

In this expression the first term in the coherent sum is the amplitude of the electronic wave emitted by the i th source in the direction defined by the angles θ and φ , and the second term sums the amplitudes of the waves scattered in the same direction by the other atoms j of the cluster, which are at the distances r_j from the source (Fig. 4). The last term takes into account diffuse scattering associated with thermal vibrations of the crystal lattice. W_j is the Debye–Waller factor, which was determined for a Debye temperature of 380 K. The total intensity of the simulated Kikuchi pattern was determined by incoherent summation of the partial contributions of the individual sources:

$$I(\theta, \varphi) \propto \sum_i I_i(\theta, \varphi) \exp\left(-\frac{z_i}{\lambda}\right). \quad (2)$$

The intensity $I(\theta, \varphi)$ was calculated at angles spaced 1° apart.

To begin the calculations we must specify a cluster that models the crystal. We selected the structural parameters describing the relative positions of the atoms in the near-surface layer under consideration on the basis of the assumption that the surface of the sample corresponds to the bulk structure of a molybdenum single crystal, whose lattice constant is 3.15 \AA . The number of atoms in the cluster was varied from a few dozen to approximately 2000 in order to find the optimum range, in which the results obtained with a

minimum number of atoms already depend weakly on the cluster size. It turned out to be necessary to use a cluster consisting of eight atomic layers, each of which contained 120 atoms and measured $31.5 \times 26.7 \text{ \AA}^2$ (10 lattice constants in the $\langle 100 \rangle$ direction and 6 interatomic distances in the $\langle 110 \rangle$ direction, respectively). These values seem reasonable, as they are comparable to λ . Finally, we note that since all the Mo atoms are found in equivalent positions in the lattice, only the central atoms of each layer were considered as emitters.

The simulation results are shown in Fig. 3c. For convenience in comparing them with experiment, they have been brought into the same form as the data in Fig. 3a. It is noteworthy that despite the simplicity of the physical model, which utilizes only isotropic sources of waves and does not take into account multiple scattering of the electrons or corrections for the sphericity of the waves, it generally describes the observed Kikuchi pattern fairly well and does not rely on any fitting parameters. The calculations reproduce essentially all the observed features of the pattern, and the disparities pertain mainly to the width and intensity of the strongest maxima (in the $[111]$ and $[010]$ directions), which are more intense and broader in the simulated pattern. This is probably due to the roughness of the description of an elastic scattering event between an electron and an atom of the solid in the plane-wave approximation. In fact, variation of the scattering amplitudes and the phase shift has the most appreciable influence on just these maxima and scarcely alters the overall appearance of the pattern. Another important reason for these disparities between theory and experiment is the multiple-scattering effects that lead to the defocusing process discussed in papers on the diffraction of Auger and photoelectrons, in which their departure from a crystal along the most densely packed rows of atoms was analyzed.

5. FOCUSING AND DEFOCUSING OF QUASIELASTICALLY SCATTERED ELECTRONS

Calculations performed in the multiple-scattering approximation^{21–23} for chains consisting of several closely spaced atoms show that the maximum degree of focusing of the emitted electrons is achieved for chains consisting of no more than three atoms. A further increase in the number of scatterers should result in weakening, and in the complete disappearance of the anisotropy of the spatial distributions of the Auger and photoelectrons, which has been termed defocusing. This conclusion was confirmed by experiments, and was not questioned until recently. However, workers have recently observed strong focusing of electrons for anomalously long chains (consisting of 10 or more atoms).^{24,25} To clear up this question, which is not only of fundamental significance, but is also important for correctly interpreting Kikuchi patterns, we measured the dependence of the degree of focusing of electrons moving along chains with different interatomic distances on the energy of the electrons. Such data enable us to analyze the role of focusing and defocusing effects, since, first, the mean free path of the electrons and, therefore, the mean escape length of quasielastically scattered electrons increase with increasing energy and, second,

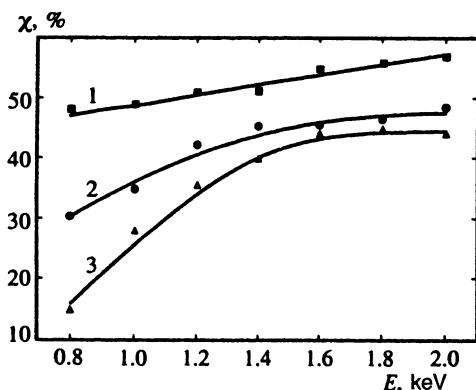


FIG. 5. Energy dependence of the degree of focusing of electrons for different directions: 1 — [111], 2 — [011], 3 — [133].

as is generally assumed, the main laws governing the focusing of electrons no longer depend strongly on their energy in the range considered (>0.8 keV).

Plots of $\chi(E)$ that illustrate the variation of the anisotropy of the spatial distributions of quasielastically scattered electrons with energy are shown in Fig. 5. The curves were obtained for three maxima in the Kikuchi pattern whose angular positions do not vary with energy, and which correspond to the densely packed [111], [011], and [133] directions of the crystal with interatomic distances d of 2.73 Å, 4.41 Å, and 6.87 Å. It must be stressed that the experimental values of χ actually characterize the magnitude of the focusing effect for these rows of atoms.

The results in Fig. 5 graphically demonstrate that focusing occurs differently in different directions. Although the degree of focusing increases with increasing energy E in all cases, the greater the interatomic spacing of the chain, the lower the initial value of χ (the value corresponding to $E=0.8$ keV) and the more pronounced the energy dependence. The latter result can be explained on a qualitative level when the mean length L of the path traversed by an electron in the solid after a quasielastic scattering event is compared with d . In fact, for focusing to occur, besides the source of the electronic wave there must be at least one scattering atom, i.e., L must be no smaller than the interatomic distance. In the [133] direction, in which the packing density of the atoms is relatively low, this condition begins to be satisfied only at an energy of ≈ 0.8 keV, which accounts for the very low value of χ for this energy and the subsequent rapid ascent of curve 3. In the more densely packed directions, the analogous "thresholds" are at lower energies, if they exist at all, and therefore the sharp increase in χ that occurs when focusing comes into play is not observed in the range investigated.

A comparison of χ in different directions reveals that the effectiveness of the electron focusing decreases with increasing interatomic distance at all energies.

The defocusing process should show up most strongly in the most densely packed rows of atoms.²³ For Mo(110) this would be the [111] direction, for which the variation of E in the range examined causes an increase in L from 8 Å to 13 Å. The monotonic course of $\chi(E)$ for this direction (the

absence of a descending branch in curve 1 of Fig. 5) graphically demonstrates that in our case defocusing is not the dominant effect, even for chains consisting of an average of 5–6 atoms. At least it does not "outweigh" the probable enhancement of focusing due to the forward peaking of the electron–atom scattering diagram resulting from the increase in energy.

6. VISUALIZATION OF THE ATOMIC STRUCTURE OF THE NEAR-SURFACE LAYERS OF A SOLID ON THE BASIS OF KIKUCHI PATTERNS

The dominant role of focusing in the formation of a Kikuchi pattern does not mean that the latter is the result of the simple superposition of the reflection maxima of electrons directed only along chains of atoms in the object under investigation. The results of the interference of the primary and scattered electronic waves clearly include not only the zero-order diffraction maxima oriented in these directions, but also maxima of higher orders, whose angular orientation depends on the energy of the electrons. Of course, they should be less intense, but can still make an appreciable contribution to the pattern and make its interpretation difficult. It is important to take this into account, if we intend to utilize Kikuchi patterns in the structural analysis of the near-surface layers of solids. In fact, when we are dealing with an object whose structure is not known *a priori*, a natural question arises: does a specific maximum in the pattern reflect a real chain of atoms or an apparent chain appearing as a result of higher-order interference features? To answer it, we can attempt to perform additional measurements to obtain data at other energies or we can carry out model calculations with variation of the structural parameters. However, both procedures are fairly tedious, and the prospects of utilizing Kikuchi patterns in surface analysis, therefore, depend decisively on how great the contribution of the higher-order diffraction maxima to the pattern actually is.

To evaluate this contribution we compared the results already considered from simulating the Mo(110) Kikuchi pattern in the single-scattering cluster approximation, which takes into account this factor, with calculations performed in a simpler model that phenomenologically describes the focusing of electrons only in the interatomic directions. In the latter case the Kikuchi pattern is regarded as an incoherent sum of the maxima in the directions joining the emitting atom to all the other scattering atoms in the cluster. In addition, the intensity of these maxima was assumed to decrease (for simplicity, according to a linear law) as the interatomic distance between the emitter and the scatterer increases. The angular distribution of the intensity within each maximum followed a normal distribution with a standard deviation of 3° , which corresponds approximately to the value of $|f_j(\theta_j)|^2$. The absorption of both the primary electrons penetrating the solid and the emitted quasielastically scattered electrons was also taken into account by the usual exponential factors $\exp(-L/\lambda)$. Model calculations were performed using the same clusters that were described during the discussion of the single-scattering approximation.

The main advantage of the proposed model is its simplicity, which makes it possible to perform a calculation of

the complete spatial distribution of the electrons within less than a minute (when a personal computer with an 80486 processor is used) even for fairly large clusters. This fact may be very significant in simulating the Kikuchi patterns of complex objects with variation of the structural parameters.

The Mo(110) Kikuchi pattern calculated using the model described is shown in Fig. 3d, in which it is represented in the same form as the other data in the figure for convenience in making comparisons. The unexpectedly good agreement between the results of the simple model calculations and experiment should, first of all, be noted. The reproduction of the main features of the Mo(110) Kikuchi pattern by both models considered, as well as the similarity between the results obtained using them (Figs. 3c and d) convincingly demonstrate the major role of the zero-order diffraction maxima in its formation. The higher-order maxima can be neglected in our case in a first approximation. Therefore, essentially all the features of the pattern correspond to interatomic directions.

Thus, the present work shows that Kikuchi patterns created by quasielastically scattered electrons directly reflect the relative orientation of the principal interatomic directions and the packing density of the atoms in them in real space (rather than in reciprocal space, as in most diffraction methods), thereby revealing the atomic structure of the near-surface region of a crystal with a thickness of several monolayers. This makes the use of Kikuchi patterns at medium electron energies very promising for structural surface analysis.

This work was performed as part of the "Surface Atomic Structures" Russian Scientific Program (Project 95-1-21).

- ¹S. A. Chambers, Surf. Sci. Rep. **16**, 261 (1992).
- ²J.-M. Pan, B. L. Maschhoff, U. Diebold, and T. E. Madey, Surf. Sci. **291**, 381 (1993).
- ³M. Erbudak, M. Hochstrasser, T. Schulthess, and E. Wetli, Philos. Mag. Lett. **68**, 179 (1993).
- ⁴M. Erbudak, M. Hochstrasser, and E. Wetli, Mod. Phys. Lett. B **8**, 1759 (1994).
- ⁵N. S. Farajev, M. V. Gomoyunova, and I. I. Pronin, Phys. Low-Dimens. Struct. **9**, 11 (1994).
- ⁶N. S. Farajev, M. V. Gomoyunova, J. Ostervalder *et al.*, Surf. Sci. **331-333**, 1446 (1995).
- ⁷H. Zhao, S. P. Tear, and A. H. Jones, Phys. Rev. B **52**, 8439 (1995).
- ⁸G. L. Robins, R. L. Gerlach, and T. N. Rodin, Appl. Phys. Lett. **8**, 12 (1966).
- ⁹R. M. Stern and H. Taub, Phys. Rev. Lett. **20**, 1340 (1968).
- ¹⁰G. Alie, E. Blanc, and D. Dufayard, Surf. Sci. **62**, 215 (1977).
- ¹¹H. Hilferink, E. Lang, and K. Heinz, Surf. Sci. **93**, 398 (1980).
- ¹²M. V. Gomoyunova, I. I. Pronin, and I. A. Shmulevitch, Surf. Sci. **139**, 443 (1984).
- ¹³Z.-L. Han, S. Hardcastle, G. R. Harp *et al.*, Surf. Sci. **258**, 313 (1991).
- ¹⁴B. L. Maschhoff, J.-M. Pan, and T. E. Madey, Surf. Sci. **259**, 190 (1991).
- ¹⁵W. F. Egelhoff, Jr., Crit. Rev. Solid State Mater. Sci. **16**, 213 (1990).
- ¹⁶S. A. Chambers, Adv. Phys. **40**, 357 (1991).
- ¹⁷C. S. Fadley, in *Synchrotron Radiation Research: Advances in Surface and Interface Science*, R. Z. Bachrach (ed.), Plenum, New York (1992), Chap. 11.
- ¹⁸I. I. Pronin, M. V. Gomoyunova, D. P. Bernatskiĭ, and S. L. Zaslavskiĭ, Prib. Tekh. Ėksp. (1), 175 (1982) [Instrum. Exp. Tech. (USSR) **25**, 198 (1982)].
- ¹⁹M. P. Seah, Surf. Interface Anal. **2**, 85 (1985).
- ²⁰M. Fink and J. Gregory, At. Data Nucl. Data Tables **14**, 39 (1974).
- ²¹H. Li and S. Y. Tong, Phys. Rev. B **32**, 2096 (1985).
- ²²M.-L. Xu and M. A. Van Hove, Surf. Sci. **207**, 215 (1989).
- ²³A. P. Kaduwela, D. J. Friedman, and C. S. Fadley, J. Electron Spectrosc. Relat. Phenom. **57**, 223 (1992).
- ²⁴M. Erbudak, T. Schulthess, and E. Wetli, Phys. Rev. B **49**, 6316 (1994).
- ²⁵S. Valeri, A. di Bona, and G. C. Gazzadi, Phys. Rev. B **50**, 14 617 (1994).

Translated by P. Shelnitz